AIAA 82-4184

Measurement of Small Normal Velocity Components in Subsonic Flows by Use of a Static Pipe

Joseph P. Nenni,* John C. Erickson Jr.,† and Charles E. Wittliff‡
Calspan Advanced Technology Center, Buffalo, N.Y.

A concept for measuring small normal velocity components in subsonic flows by use of a static pipe has been developed and tested. A theory is presented which allows one to relate measurements of the difference of static pressures across a static pipe in a slightly disturbed flow to the axial derivative of the velocity component normal to the pipe. This derivative may be integrated, after fixing the constant of integration, to give the normal velocity component distribution along the pipe. The theory is restricted to small normal velocity components relative to the main freestream flow which is aligned with the pipe axis. The theoretical development presented here is primarily concerned with two-dimensional disturbance fields, but results are given for three-dimensional disturbance fields also. An experimental application of the concept to measure the disturbance fields arising in a two-dimensional wind tunnel is described. These experiments show how the present static-pipe concept can be used in a practical experimental situation.

Nomenclature

b	= semiminor axis of ellipse
c	= chord length or disturbance characteristic length
c_p	= pressure coefficient
d	= semimajor axis of ellipse
E	= ratio of minor to major axis of ellipse
G_1, G_2	= functions of x in inner solution
h	= distance from tunnel centerline to pipe axis
K_i	= pressure coefficient on pipe surface at $\omega = (2i-1)\pi/4$
M_∞	= freestream Mach number
p_∞	= freestream static pressure
P	= line doublet strength
r	$= \sqrt{z^2+y^2}$
R	= pipe radius
$\mathfrak{R}$	= radial independent variable (inner variable)
$\mathfrak{S}$	= pipe surface shape function
U_∞	= freestream velocity
u_1, v_1	= disturbance field velocities in x and y directions, respectively
$\hat{u}_1, \hat{v}_1$	= disturbance velocities normalized by U_∞
x_R	= reference station for $\hat{v}_1$
x,y,z	= Cartesian coordinates scaled by c
Y,Z	= inner variables in cross-flow plane
β	$= \sqrt{1-M_\infty^2}$
δ	$= R/c$
ϵ	= small parameter
σ_1	= gage function in inner solution
ϕ^T	= total velocity potential
ϕ_1, ϕ_2	= decomposition of velocity potential introduced in Eq. (1)
ϕ_{1i}	= coefficients in Taylor series expansion of ϕ_1
Φ_i	= terms in expansion of inner solution
ω	= azimuthal independent variable

Received Feb. 20, 1981; revision received Dec. 14, 1981.

*Senior Engineer, Aerodynamic Research Department. Member AIAA.

†Principal Engineer, Aerodynamics Research Dept.; now Senior Research Engineer, Propulsion Wind Tunnel Facility, Calspan Field Services Inc. AEDC Division, Arnold Air Force Station, Tenn. Member AIAA.

‡Principal Engineer, Aerodynamic Research Department. Member AIAA.

Introduction

STATIC pipes long have been used in the calibration of transonic and subsonic wind tunnels. Although their use has been limited principally to measurements of axial Mach number perturbations and static pressure uniformity, further analysis reveals that they may be used to measure normal velocity perturbations accurately also. This capability provides a relatively inexpensive and rugged means of measuring normal velocity components and may compete favorably with hot wires, flow-angle probes, or LDV systems for some applications. The present concept was developed for ventilated-wall, transonic wind tunnel use.[1] The static-pipe development is reported more fully in Ref. 2.

The theory developed in the following sections assumes that the freestream flow is uniform and aligned with the pipe axis and has a small nonuniform irrotational disturbance field imposed upon it. The disturbance field amplitude scales with a small parameter denoted by ϵ. It is further assumed that the pipe radius R is small compared to a characteristic length c of the disturbance field (say, for instance, that the disturbance field is generated by an airfoil of chord length c). The ratio R/c is denoted by δ. An expression for the pressure coefficient on the pipe surface is determined which is second-order accurate in terms of the small parameters ϵ and δ. The method of matched asymptotic expansions[3] is used to derive a velocity potential for the total disturbance flowfield in the presence of the pipe. The velocity potential is determined through third order in terms of the small quantities involved. Only the second-order results are used; the third-order solution is developed mainly to ensure that all second-order terms are properly accounted for.

The main body of the theory presented here is restricted to a two-dimensional disturbance field for exposition purposes. The extension to a three-dimensional disturbance field is straightforward and the results are given. Also, the basic theoretical development is for circular cross-section pipes; but, the problem for elliptical cross-section pipes in a two-dimensional disturbance field has also been solved and the results are presented. Finally, transonic wind-tunnel experiments are described as an application of the theory for two-dimensional disturbances. This gives an example of application of the present static-pipe concept in a practical experimental situation.

Theoretical Analysis for Two-Dimensional Disturbance Fields

Consider the pressure induced on a static pipe which is immersed in a flow mainly aligned with the pipe axis as shown

in Fig. 1. The flow is composed of a uniform flow of velocity U_∞, aligned with the pipe axis, plus an initially two-dimensional disturbance (function of x and y) that scales with a small parameter ϵ. The viscous boundary-layer thickness on the pipe is assumed small compared to the radius of the pipe so that the surface pressures on the pipe may be calculated by an inviscid theory. Further, since only small flow inclinations to the pipe axis are being considered, vortex formation on the leeside of the pipe will be ignored. The flow is assumed to be subsonic but compressible such that the Prandtl-Glauert approximation applies. The total velocity potential will be assumed to be of the following form

$$\phi^T(x,y,z) = U_\infty x + \epsilon U_\infty [\phi_1(x,y) + \phi_2(x,y,z)] \tag{1}$$

Here all of the spatial variables have been scaled by c and ϕ_1 corresponds to the initial two-dimensional disturbance which is sought in the analysis. Then ϕ_2 corresponds to the three-dimensional interaction between the pipe and the disturbance field. The desired x and y disturbance velocity components associated with ϕ_1 will be denoted by u_1 and v_1, respectively. The pipe surface is described by

$$\mathcal{S} = y^2 + z^2 - \delta^2 = 0$$

where $\delta = R/c$, the nondimensional pipe radius.

In the Prandtl-Glauert approximation, the total potential satisfies

$$(1-M_\infty^2)\phi^T_{xx} + \phi^T_{yy} + \phi^T_{zz} = 0 \tag{2}$$

subject to the boundary condition

$$\nabla\phi^T \cdot \nabla\mathcal{S} = 0 \text{ on } \mathcal{S} = 0 \tag{3}$$

It is assumed that δ is a small parameter, that is, $\delta \ll 1$, and the technique of matched asymptotic expansions[3] is used to find the appropriate expansion for ϕ_2. As $\delta \to 0$, the pipe shrinks to a line. Tentatively, then, the outer solution is represented by a line doublet distribution plus a line source distribution, viz.,

$$\phi^{T,0} \sim U_\infty x + \epsilon U_\infty \left\{ \phi_1(x,y) + \frac{\delta^2}{4\pi}\frac{y}{r^2}\int_{-\infty}^{\infty} \frac{P(x_0)(x-x_0)}{[(x-x_0)^2+\beta^2 r^2]^{1/2}}\,dx_0 + \frac{\sigma_1(\delta)}{2\pi}\int_{-\infty}^{\infty} \frac{Q(x_0)}{[(x-x_0)^2+\beta^2 r^2]^{1/2}}\,dx_0 \right\} \tag{4}$$

where $r^2 = y^2 + z^2$. The doublet strength $P(x_0)$ will be determined by matching with an inner solution to first order in δ. The source term (second integral expression) is not needed to first order in δ, so both its strength $Q(x_0)$ and gage function $\sigma_1(\delta)$ will be determined by matching with higher-order inner solutions.

Inner Solution

The inner problem is obtained by stretching the coordinates normal to the pipe by

$$Y = y/\delta, \qquad Z = z/\delta$$

Then $\phi_1(x,y)$ must be expanded accordingly as

$$\phi_1(x,\delta Y) = \phi_{10}(x) + \delta\phi_{11}(x)\,Y + \delta^2\phi_{12}(x)\,Y^2 + 0(\delta^3) \tag{5}$$

It should be noted that $d\phi_{10}/dx$ is proportional to the desired streamwise disturbance velocity component u_1 along the pipe centerline and $\delta\phi_{11}$ is proportional to the normal component v_1 there.

Next, it is assumed that the total inner solution is of the form

$$\phi^{T,I} = U_\infty x + \epsilon U_\infty \{\phi_{10} + \delta(\phi_{11}Y + \Phi_2) + \delta^2(\phi_{12}Y^2 + \Phi_3) + 0(\delta^3, \delta^3 \ell n\delta)\} \tag{6}$$

The ordering of the terms in this solution form is dictated by Eq. (5) and differs slightly from the conventional slender-body expansion. It can be shown that both Φ_2 and Φ_3 satisfy the two-dimensional Laplace equation in the cross-flow plane, while the boundary condition, Eq. (3), reduces to

$$Y\Phi_{2_Y} + Z\Phi_{2_Z} = -Y\phi_{11} \tag{7}$$

and

$$Y\Phi_{3_Y} + Z\Phi_{3_Z} = -2Y^2\phi_{12} \tag{8}$$

both on

$$Y^2 + Z^2 - 1 = 0$$

Physically, it may be seen that the problem for Φ_2 corresponds to that of a cylinder with unit radius immersed in a flow of magnitude ϕ_{11}. The corresponding solution is

$$\Phi_2 = \phi_{11}Y/(Y^2+Z^2) + G_1(x) \tag{9}$$

or, in polar coordinates ($Y = -\Re\cos\omega$, $Z = -\Re\sin\omega$),

$$\Phi_2 = -\phi_{11}\cos\omega/\Re + G_1(x) \tag{10}$$

Matching with the outer solution will be carried out subsequently to obtain $G_1(x)$ and $P(x)$.

The solution for Φ_3 is found most easily using polar coordinates, in terms of which Eq. (8) becomes

$$\Phi_{3_\Re} = -2\phi_{12}\cos^2\omega \tag{11}$$

on $\Re = 1$, where the subscript $\Re$ denotes differentiation with respect to $\Re$. After suitable manipulation, Poisson's integral formula may be used to solve for Φ_3. First, let

$$\Phi_3 = \Phi_3^B + K\ell n\Re + G_2(x) \tag{12}$$

where K is a constant which will be chosen later. Then

$$\Phi_{3_\Re} = \Phi^B_{3_\Re} + (K/\Re)$$

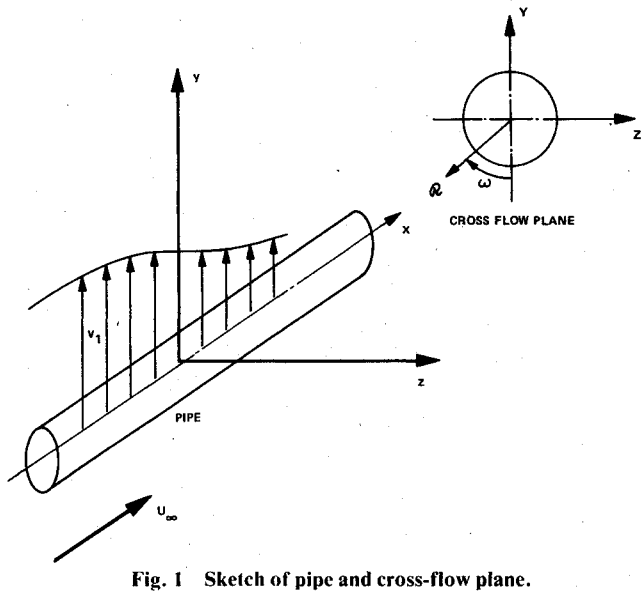

Fig. 1 Sketch of pipe and cross-flow plane.

and Eq. (11) becomes

$$-2\phi_{12}\cos^2\omega = \Phi^B_{3_{\mathcal{R}}} \mid_{\mathcal{R}=1} + K$$

or

$$\Phi^B_{3_{\mathcal{R}}} \mid_{\mathcal{R}=1} = -(K + 2\phi_{12}\cos^2\omega)$$

In order to use the Poisson integral formula, K is chosen such that

$$\int_0^{2\pi} \Phi^B_{3_{\mathcal{R}}} \mid_{\mathcal{R}=1} \mathrm{d}\omega = 0$$

which leads to $K = -\phi_{12}$, so that

$$\Phi^B_{3_{\mathcal{R}}} \mid_{\mathcal{R}=1} = \phi_{12}(1 - 2\cos^2\omega) \tag{13}$$

Finally, by Poisson's integral formula (see Ref. 4, p. 254),

$$\Phi^B_3 = -\frac{\phi_{12}}{2\pi}\int_0^{2\pi}(1-2\cos^2\omega_0)\ln[1 - 2\mathcal{R}\sin(\omega_0 - \omega) + \mathcal{R}^2]\,\mathrm{d}\omega_0 \tag{14}$$

The function Φ_3 is now determined up to a function of x, $G_2(x)$ say, and possible eigensolutions that are required to match with the outer solution.

Matching and Final Solution Forms

The outer solution, Eq. (4), when written in terms of the inner variables, becomes

$$\phi^{T,0} = U_\infty x + \epsilon U_\infty \left\{\phi_1(x,\delta Y) + \frac{\delta}{4\pi}\frac{Y}{\mathcal{R}^2}\int_{-\infty}^{\infty}\frac{P(x_0)(x-x_0)}{[(x-x_0)^2 + \delta^2\beta^2\mathcal{R}^2]^{1/2}}\,\mathrm{d}x_0 + \frac{\sigma_1(\delta)}{2\pi}\int_{-\infty}^{\infty}\frac{Q(x_0)}{[(x-x_0)^2 + \delta^2\beta^2\mathcal{R}^2]^{1/2}}\,\mathrm{d}x_0\right\} \tag{15}$$

When this equation is expanded for small δ, using Eq. (5), the result is

$$\phi^{T,0} \sim U_\infty x + \epsilon U_\infty \left\{\phi_{10}(x) + \delta\phi_{11}Y + \delta^2\phi_{12}Y^2 + \frac{\delta Y}{4\pi\mathcal{R}^2}\left[\int_{-\infty}^{x} P(x_0)\,\mathrm{d}x_0 - \int_x^{\infty} P(x_0)\,\mathrm{d}x_0\right] + \frac{\sigma_1(\delta)}{2\pi}\left[-Q(x)2\ln\mathcal{R} - Q(x)\ln\delta^2\beta^2 + \int_{-\infty}^{x} Q'(x_0)\ln 2(x-x_0)\,\mathrm{d}x_0 - \int_x^{\infty} Q'(x_0)\ln 2(x_0-x)\,\mathrm{d}x_0\right] + O(\delta^3, \delta\sigma_1)\right\} \tag{16}$$

where a prime indicates differentiation with respect to x.

The inner solution, Eq. (6), when written in terms of the outer variables and using the results in Eqs. (10) and (14), becomes

$$\Phi = U_\infty x + \epsilon U_\infty \left\{\phi_{10} + \left[\phi_{11}y + \frac{\delta^2\phi_{11}y}{r^2} + \delta G_1(x)\right] + \left[\phi_{12}y^2 - \delta^2\phi_{12}\ln\left(\frac{r}{\delta}\right) - \frac{\delta^2\phi_{12}}{2\pi}\int_0^{2\pi}(1-2\cos^2\omega')\times\ln\left[1 - 2\left(\frac{r}{\delta}\right)\sin(\omega'-\omega) + \left(\frac{r}{\delta}\right)^2\right]\mathrm{d}\omega' + \delta^2 G_2(x)\right]\right\} \tag{17}$$

When this equation is expanded for small δ, the result is

$$\Phi \sim U_\infty x + \epsilon U_\infty \left\{\phi_{10} + \left[\phi_{11}y + \frac{\delta^2\phi_{11}y}{r^2} + \delta G_1(x)\right] + \left[\phi_{12}y^2 - \delta^2\phi_{12}\ln\left(\frac{r}{\delta}\right) + \delta^2 G_2(x)\right] + O(\delta^4)\right\} \tag{18}$$

Matching Eqs. (16) and (18) results in

$$G_1(x) = 0, \qquad P(x) = 2\pi\phi'_{11}(x)$$

to complete the solution for the line doublet distribution, and

$$\sigma_1 = \delta^2, \qquad Q(x) = \pi\phi_{12}(x)$$

$$G_2(x) = -\phi_{12}(x)\ln\delta\beta + \frac{1}{2}\int_{-\infty}^{x}\phi'_{12}(x_0)\ln 2(x-x_0)\,\mathrm{d}x_0 - \frac{1}{2}\int_x^{\infty}\phi'_{12}(x_0)\ln 2(x_0-x)\,\mathrm{d}x_0$$

to complete the solution for the line source distribution. Inspection of the first term of $G_2(x)$ indicates that an additional term of order $\delta^2\ln\delta$ should have been assumed in the inner expansion of Eq. (6). However, consideration of the boundary conditions quickly shows that this additional term is a function only of x, and is precisely the first term of $G_2(x)$. Furthermore, no eigensolutions are necessary to perform the matching.

Pressure Coefficient

The pressure coefficient may be calculated from the inner solution and, to second order in the small parameters (i.e., retaining ϵ^2, δ^2, and $\epsilon\delta$), is

$$c_p = -2\epsilon\phi'_{10} - 2\epsilon\delta(\phi'_{11}Y + \Phi_{2_X}) - \epsilon^2[(\phi'_{10})^2(1-M_\infty^2) + \Phi_{2_Z}^2 + (\phi_{11} + \Phi_{2_Y})^2] \tag{19}$$

Now using this expression and measuring the pressure coefficient at various azimuthal locations for a fixed axial location on the pipe surface, it is possible to combine the measured values so as to isolate the desired quantities u_1 and v_1. On the pipe surface c_p is only a function of x and ω, $c_p = c_p(x,\omega)$. Considering measurements on the top and bottom of the pipe (see Fig. 1), let

$$c_{p_1} = c_p(x,0) \qquad c_{p_2} = c_p(x,\pi)$$

Then from Eq. (19) it follows that

$$c_{p_1} = -2\hat{u}_1(x) - \beta^2 \hat{u}_1^2(x) + 4\delta \hat{v}_1'(x) \tag{20}$$

$$c_{p_2} = -2\hat{u}_1(x) - \beta^2 \hat{u}_1^2(x) - 4\delta \hat{v}_1'(x) \tag{21}$$

where $\hat{u}_1 = u_1/U_\infty$ and $\hat{v}_1 = v_1/U_\infty$ are the normalized disturbance velocities on the pipe centerline due to the initial disturbance field and are of order ϵ. Combining Eqs. (20) and (21) yields

$$\hat{u}_1(x) = -\frac{1}{\beta^2}\left\{1 - \left[1 - \beta^2 \frac{(c_{p_1} + c_{p_2})}{2}\right]^{1/2}\right\} \tag{22}$$

$$\hat{v}_1' = (c_{p_1} - c_{p_2})/8\delta \tag{23}$$

Assuming that $\hat{v}_1$ is known at a reference station x_R, Eq. (23) may be integrated to give

$$\hat{v}_1(x) = \hat{v}_1(x_R) + \int_{x_R}^{x} \hat{v}_1'(x_0)\,dx_0 \tag{24}$$

Equations (22) and (24) are the major results of the analysis and they show that if $\hat{v}_1$ can be measured at a suitable reference point, the pressure distributions along the top and bottom of the pipe may be used to determine $\hat{v}_1(x)$ and $\hat{u}_1(x)$. The measurement of $\hat{v}_1(x_R)$ would have to be made by an alternative measuring technique or x_R would have to be chosen where $\hat{v}_1(x_R)$ is known to be zero. If a third pressure measurement is made on the side of the pipe ($\omega = \pi/2$ or $3\pi/2$) it is possible to determine $\hat{v}_1$ directly from the pressure measurements and thus eliminate the requirement for independent measurement of $\hat{v}_1(x_R)$. This extension of the analysis is given in Ref. 2.

The foregoing analysis can also be used for noncircular cross-section static pipes. For example, consider the pipe to have an elliptical cross section with major axis parallel to the y direction. The cross-sectional shape is given by $y^2/d^2 + z^2/b^2 = 1$. Recall that y and z are scaled by c and therefore b and d must be so scaled. In this case d is chosen as the small parameter and let $E = b/d < 1$. The previous analysis may be repeated using the cross-flow solution about an ellipse in place of the solution for a circular cylinder. Then the results corresponding to Eqs. (22) and (23) are

$$\hat{u}_1(x) = -\frac{1}{\beta^2}\left\{1 - \left[1 - \beta^2 \frac{(c_{p_1} + c_{p_2})}{2}\right]^{1/2}\right\} \tag{25}$$

$$\hat{v}_1' = \frac{c_{p_1} - c_{p_2}}{4(1+E)d} \tag{26}$$

This last expression may be integrated to obtain an expression similar to Eq. (24). Note that only the expression for $\hat{v}_1'$ in terms of the pressure difference is modified from the results for a circular cylinder. For a fixed $\hat{v}_1'$ and equal cross-sectional areas of the pipe, Eqs. (23) and (26) may be used to show that the elliptical pipe would produce a larger difference in pressure coefficient across the pipe by the factor $(1+E)/(2\sqrt{E})$ which is greater than one for $0 < E < 1$.

Three-Dimensional Disturbance Fields

In case the initial disturbance field associated with ϕ_1 is three dimensional, the preceding analysis for the circular pipe is extended easily. In this case the inner solution easily is decoupled into a term dependent upon v_1 similar to Eq. (9) plus a like term dependent upon w_1, the z component of the disturbance velocity at the pipe centerline. The details of this analysis are presented in Ref. 2; only the results will be given here. In terms of the initial disturbance velocities at the pipe centerline, the expression for the pressure coefficient on the pipe surface is

$$c_p(x,\omega) = -2\hat{u}_1 - \beta^2 \hat{u}_1^2 + 4\delta[\hat{v}_1' \cos\omega + \hat{w}_1' \sin\omega] - 4[\hat{v}_1 \sin\omega - \hat{w}_1 \cos\omega]^2 \tag{27}$$

For the three-dimensional case, one procedure is to measure the pressure at four azimuthal locations at each axial station. The procedure using $\omega = 0$, $\pi/2$, π and $3\pi/2$ is given in Ref. 2; however, the choice $\omega = \pi/4$, $3\pi/4$, $5\pi/4$, and $7\pi/4$ subsequently has been found to require somewhat less data processing and is presented here. Let

$$c_p\left(x, \frac{\pi}{4}\right) \equiv K_1 \qquad c_p\left(x, \frac{3\pi}{4}\right) \equiv K_2$$

$$c_p\left(x, \frac{5\pi}{4}\right) \equiv K_3 \qquad c_p\left(x, \frac{7\pi}{4}\right) \equiv K_4$$

Combining these measurements the following relations are obtained.

$$\hat{w}_1' = (K_1 + K_4 - K_2 - K_3)\sqrt{2}/16\delta \tag{28a}$$

$$\hat{v}_1' = (K_1 - K_4 + K_2 - K_3)\sqrt{2}/16\delta \tag{28b}$$

These expressions may be integrated as in the two-dimensional disturbance case with the convenience that only one reference measurement of either $\hat{v}_1$ or $\hat{w}_1$ is necessary because the product of the disturbance velocities is related by

$$\hat{v}_1 \hat{w}_1 = \frac{1}{16}(K_1 - K_4 + K_3 - K_2) \tag{29}$$

Once $\hat{v}_1$ and $\hat{w}_1$ are known, $\hat{u}_1$ may be obtained from

$$\hat{u}_1 = -\frac{1}{\beta^2} + \frac{1}{\beta^2}\left\{1 - \beta^2\left[\frac{K_1 + K_2 + K_3 + K_4}{4} + 2(\hat{v}_1^2 + \hat{w}_1^2)\right]\right\}^{1/2} \tag{30}$$

The selection of the azimuthal locations for the pressure orifices on the pipe may be optimized to suit the particular needs of a given experimental situation. The range of selection is practically limitless. In addition to the choices just discussed, the case with three equally spaced orifices may be attractive for some circumstances. In this case one may obtain a coupled pair of nonlinear ordinary differential equations for $\hat{v}_1$ and $\hat{w}_1$ that may be integrated by standard means if reference values of both $\hat{v}_1$ and $\hat{w}_1$ are independently measured. In connection with normal usage of static pipes the analyses presented above show that the average value of pressure coefficients measured at any axial station may be zero yet the flow still may be disturbed. Disturbances which are uniform in the axial direction are particularly deceptive in this regard.

Static-Pipe Application

The first application of the static-pipe technique for determining the velocity component normal to the pipe was made in recent transonic wind-tunnel experiments.[2] In early experiments in the Calspan 1-ft transonic wind tunnel,[1,5-7] local flow inclination near the tunnel walls was measured by a total of 18 aerodynamic probes and the local static pressure by a pair of static pipes with rows of orifices at $\omega = \pi/2$. The probes, which are described fully in Ref. 6, consist of two side-by-side tubes which are chamfered at 45 deg in opposite senses to one another to achieve pitch angle sensitivity. The

Table 1 Empty tunnel flow measurements of $\hat{u}_1$

Mach number	Upper pipe Mean	Upper pipe Std. dev.	Lower pipe Mean	Lower pipe Std. dev.	Both pipes Mean	Both pipes Std. Dev.
0.55	−0.0017	±0.0016	−0.0003	±0.0021	−0.0010	±0.0020
0.75	−0.0008	±0.0016	−0.0006	±0.0017	−0.0007	±0.0016
0.85	−0.0008	±0.0025	−0.0008	±0.0024	−0.0008	±0.0024
0.95	−0.0000	±0.0046	−0.0014	±0.0036	−0.0007	±0.0042

velocity component $\hat{v}_1$ is determined from the pressure difference between the tubes by use of appropriate probe calibrations.[6] The static pressure measured on the side orifices of the static pipes is related to $\hat{u}_1$ and $\hat{v}_1$ by Eq. (19), namely,

$$c_{p_0} = c_p\left(x, \frac{\pi}{2}\right) = -2\hat{u}_1(x) - \beta^2\hat{u}_1^2(x) - 4\hat{v}_1^2(x)$$

which can be solved to give

$$\hat{u}_1(x) = -\frac{1}{\beta^2}\{1 - [1 - \beta^2(c_{p_0} + 4\hat{v}_1^2(x))]^{1/2}\} \qquad (31)$$

In the early experiments, however, the linearized version of Eq. (31) was used, namely, $\hat{u}_1(x) = -c_{p_0}/2$, thus incurring a small error in the determination of $\hat{u}_1$ at the axial location of the model.

Blockage and wake interference considerations restrict the number of flow-angle probes that can be installed. The resulting small number of probes limits the definition of the distributions of $\hat{v}_1$ at the axial locations near the model where $\hat{v}_1$ varies rapidly. Moreover, the small probes that must be used are very sensitive to contamination from oil present in the stream of the tunnel. Finally, the probes require extensive and recurring calibrations. Consequently, the static-pipe technique described herein was developed to overcome these limitations.

On the basis of available materials and ease of construction, it was decided that the new pipes would have a 0.016-m o.d. circular cross section with diametrically opposed orifices on the top and bottom of the pipes in the vicinity of the model, i.e., at $\omega = 0$ and π. The pipes were 2.44-m long with their noses located well upstream of the test section in the contraction region of the nozzle. The experiments were performed with an NACA 0012 airfoil model in the tunnel. The chord is 0.102 m, so $\delta = 0.0781$. There are 18 pairs of opposed orifices on the pipes extending 0.229-m upstream (to $x = -2.25$) and 0.279-m downstream (to $x = 2.75$) of a point 0.018-m behind the airfoil leading edge. These dual orifices span the region where the static pressure differences are expected to be equal to or greater than the resolution capability of the transducers. Upstream and downstream of this region, the static pipes have orifices which extend the full length of the test section along the side of the pipe facing the model. The most forward static pressure orifice on each pipe (located at the beginning of the test section) is connected to a manifold and the reading is taken to be the freestream static pressure p_∞. All remaining 33 pressures on the model sides of the pipes are measured relative to p_∞. In addition, the differential pressures between the 18 opposing pairs of orifices on each pipe are measured. The differential pressure transducers used have a probable error of 6.9 Pa or less, and the readout system has a resolution of 6.9 Pa. For reference, p_∞ in the experiments varies with Mach number and ranges from 56,000 Pa at $M_\infty = 0.55$ to 30,000 Pa at $M_\infty = 0.9$. The pipes are mounted with their centerlines located a distance h of 0.102-m above and below the test section centerline, so that $h/c = \pm 1.0$.

Table 2 Differential measurements across pipe of $c_{p_1} - c_{p_2}$ in empty tunnel

Mach number	Upper pipe Mean	Upper pipe Std. dev.	Lower pipe Mean	Lower pipe Std. dev.
0.55	+0.0004	±0.0024	+0.0008	±0.0022
0.75	+0.0014	±0.0024	−0.0010	±0.0016
0.85	+0.0014	±0.0026	−0.0010	±0.0018
0.95	+0.0016	±0.0030	−0.0012	±0.0030

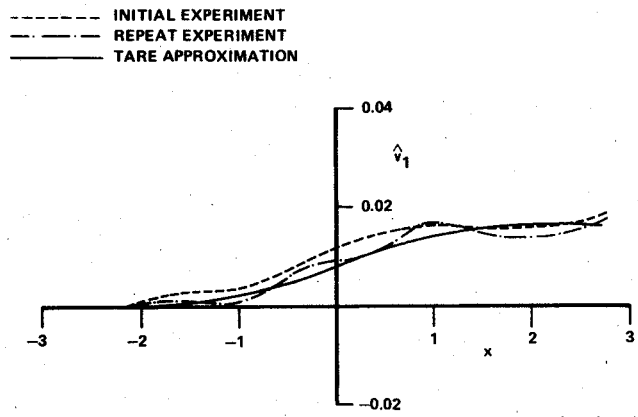

Fig. 2 Apparent normal velocity measured by upper static pipe in uniform, parallel flow without model, $M_\infty = 0.8$, $h/c = 1.0$.

The first experiments were a series of tests performed without the airfoil model installed in the tunnel to provide probe and pipe calibration data. For convenience, these will be referred to as empty-tunnel tests. In these experiments, a uniform flow in the tunnel was established so that $c_{p_1} = 0$ was obtained at selected pipe orifices. The data at all orifices were then measured and reduced according to Eqs. (22) and (23) to determine $\hat{u}_1$ and $\hat{v}_1$ for each test Mach number. The mean values and standard deviations of $\hat{u}_1$ along the pipes are presented in Table 1 for representative cases. The difference of the mean values from zero is significantly less than the standard deviations (with one exception—the upper pipe at $M_\infty = 0.55$). The flow quality at Mach numbers of 0.55, 0.75, and 0.85 is comparable and the standard deviations are all about ±0.0020. At $M_\infty = 0.95$, the standard deviation of all the data is approximately ±0.0040; however, this is due to deviations at the far upstream and downstream ends of the test section. Over the central 0.508-m distance near the model location, the standard deviation is ±0.0022, which is in good agreement with the lower Mach number results.

The pressure differentials measured by the opposing pairs of orifices have also been analyzed. The mean values and standard deviations of $c_{p_1} - c_{p_2}$ along the pipes are presented in Table 2 for the same representative cases. They exhibit mean values of about ±0.0010 with standard deviations of ±0.0020. These mean values are small and comparable to those for the overall flow, as in Table 1. However, the fact that the means are not zero has a significant implication on the determination of $\hat{v}_1$ with the pipes. The empty-tunnel differential pressure data were reduced, spline fit, and in-

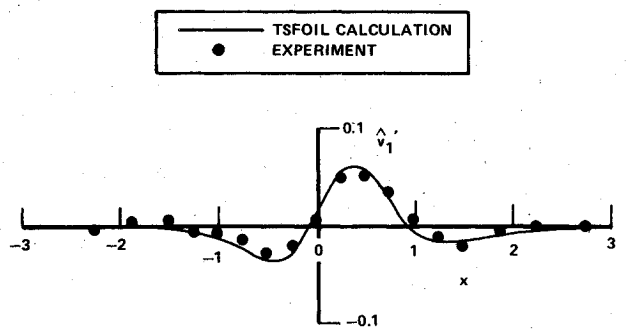

a) Lower pipe, $h/c = -1.0$.

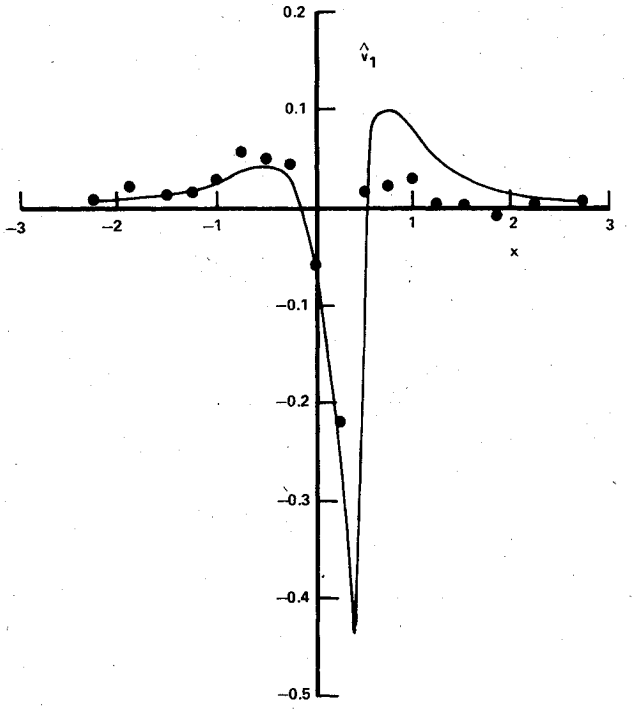

b) Upper pipe, $h/c = 1.0$.

Fig. 3 Static pipe measurements of axial derivative of normal velocity, $M_\infty = 0.8$, $\alpha = 4$ deg.

tegrated according to Eq. (24) from $x = -2.25$ to 2.75 with $\hat{v}_I(-2.25) = 0$. The resulting cumulative effect of the nonzero pressure differentials of one predominant sign was significant. This can be seen in Fig. 2, where the results at the upper pipe for two different empty-tunnel runs at $M_\infty = 0.8$ are presented. The integrated values are comparable in magnitude to the normal velocity measurements that are encountered experimentally. All empty-tunnel data were examined in this way. It was found that the upper pipe data integrated in all cases to give positive $\hat{v}_I$ distributions of roughly the magnitude shown in Fig. 2. At the lower pipe, however, the results were different and contradictory. That is, some cases integrated to give positive $\hat{v}_I$ (of smaller magnitude than in Fig. 2) and some to give negative $\hat{v}_I$. Indeed, at the lower pipe $\hat{v}_I$ was positive in one run and negative in the other for the experiments shown in Fig. 2.

Several possible causes of this phenomenon were examined in Ref. 2. It was concluded that the flow is in fact uniform, as indicated by the small measured $\hat{u}_I$ variations, and the anomalies in the pipe differential measurements are an artifact of the detailed geometry of the individual pipes, since the characteristics of each differ. Consequently, this effect at the upper pipe was treated as a tare reading to be subtracted at each orifice from the measured $\hat{v}_I'$. The integrated $\hat{v}_I$ from the assumed tare is shown in Fig. 2 and appears to provide a reasonable approximation to the experimental curves for both empty-tunnel runs at this M_∞. No tare was used at the lower pipe because it averaged nearly to zero for all runs considered.

An example of the use of the new static-pipe technique in conjunction with the flow-angle probes in experiments in the Calspan 1-ft tunnel for the 0.102-m chord NACA 0012 airfoil model at $M_\infty = 0.8$ and an angle of attack α of 4 deg. The data for $\hat{v}_I'(x)$, as calculated by Eq. (23) from the static-pipe measurements with the upper pipe tare correction included, are presented in Figs. 3a and b for the lower and upper pipes, respectively. The estimated unconfined-flow distributions calculated by the TSFOIL computer code[8] are also given in Fig. 3, but are for reference only since there is no reason to believe that the data represent unconfined flow conditions.

The data at the lower pipe will be discussed first since there was no shock wave below the airfoil. The $\hat{v}_I'(x)$ data of Fig. 3a were fit by a cubic spline over the entire interval from $x = -2.25$ to $x = 2.75$ for which measurements were made. This spline fit was then integrated according to Eq. (24) with $\hat{v}_I(-2.25)$ temporarily set equal to zero to give the dashed curve shown in Fig. 4a. The actual reference velocity $\hat{v}_I(-2.25)$ was then established by a least-squares fit of the integrated curve to the four probe measurements of $\hat{v}_I$ at $x = -1.48$, -1.12, 0.83, and 2.52 in Fig. 4a. The resulting curve was then faired upstream through the first three probe measurements and downstream through the last two to arrive at the final $\hat{v}_I(x)$ distribution shown in Fig. 4a.

The theory as developed herein is not applicable when the disturbance causes formation of a supersonic pocket followed by a shock such as occurs at the upper pipe in this example. This could be remedied by devising another expansion procedure to apply locally in the vicinity of the shock. However, a more utilitarian viewpoint has been adopted wherein it is assumed that the theoretical development presented here applies independently upstream and downstream of the shock. Then separate estimates of $\hat{v}_I$ are constructed based upon selection of different $\hat{v}_I(x_R)$ and x_R values on either side of the shock. The location of the shock in this experiment is apparent from the $\hat{u}_I(x)$ data and the schlieren observations. Accordingly, the data were fit by a cubic spline from the first measured point at $x = -2.25$ to the last point before the shock at $x = 0.25$. The spline fit was then integrated up to $x = 0.25$ with $\hat{v}_I(-2.25)$ temporarily set equal to zero to give the dashed curve in Fig. 4b. The actual reference velocity was chosen by adjusting the integrated curve to pass through the probe measurement at $x = -1.95$ and the curve was faired upstream through the first two probe measurements. Downstream of the shock a similar procedure was used. The $\hat{v}_I'(x)$ data from $x = 0.50$ to $x = 2.75$ were spline fit and then integrated upstream from a temporary reference value of zero at $x = 2.75$ to $x = 0.50$ to give the other branch of the dashed curve in Fig. 4b. This branch was adjusted by a least-squares fit to the two probe measurements at $x = 1.25$ and 2.05. It was then faired downstream through the last three probe measurements. In the vicinity of the shock, the upstream and downstream branches were simply extrapolated until they intersect to give the final $\hat{v}_I(x)$ distribution in Fig. 4b.

It is clear that additional measurements in the vicinity of the shock wave would be highly desirable, but this was not possible with the present configuration. In fact, it would be difficult to construct a pipe with sufficient measurement orifices to cover all shock locations for a wide range of models and operating conditions. Accordingly, an alternative such as pipes which translate streamwise may offer a better possibility for more complete definition of the distributions in future applications. Despite this limitation of the existing configuration, the new static-pipe technique, in conjunction with probes, does provide an improved technique for determining the normal velocity distributions compared to that of the probes alone.

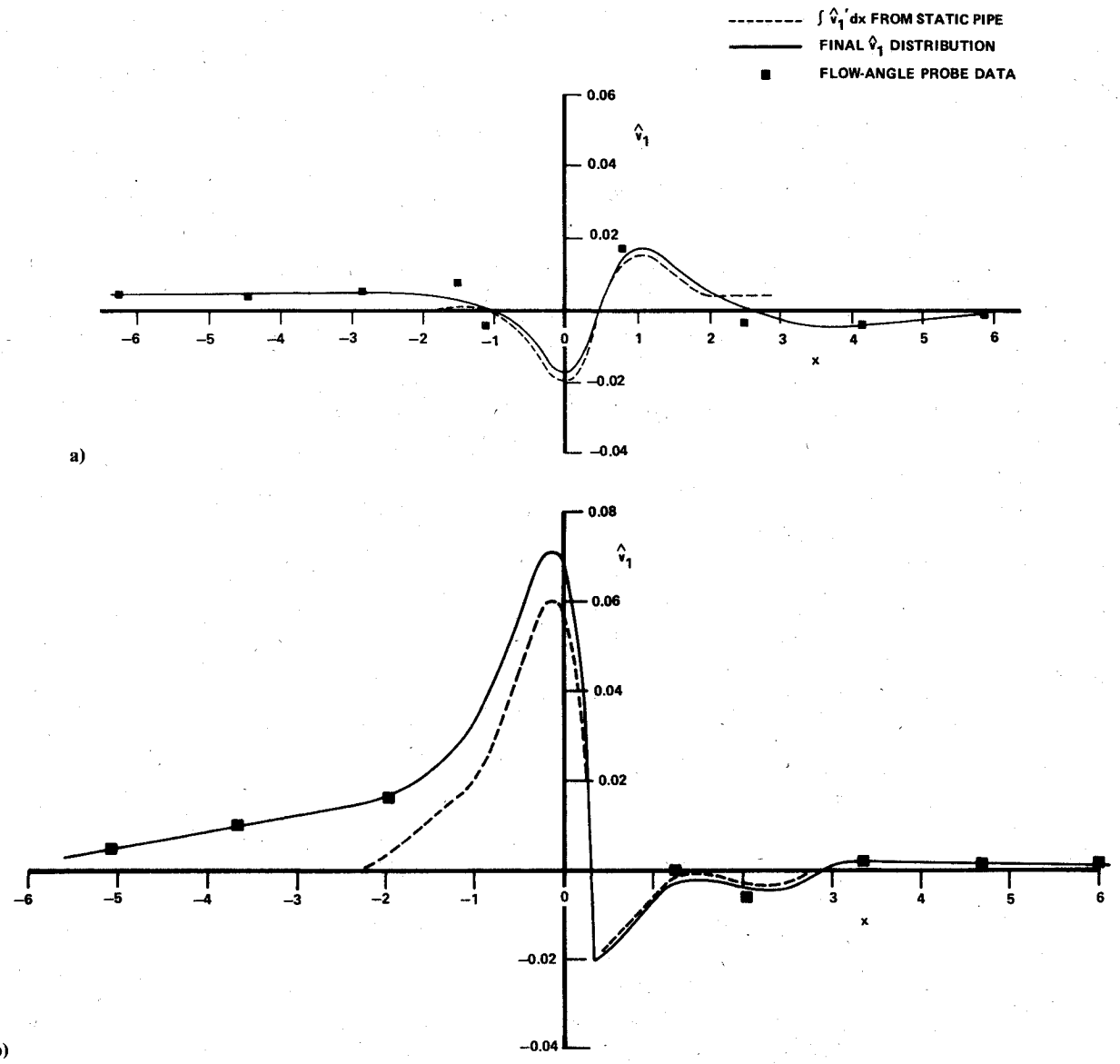

Fig. 4 Normal velocity determined from static pipes and flow-angle probes, $M_\infty = 0.8$, $\alpha = 4$ deg; a) lower pipe, $h/c = -1.0$, and b) upper pipe, $h/c = 1.0$.

Conclusions

A method has been developed to use static pipes for the measurement of small normal velocity components in subsonic flows. The theoretical development presented allows one to use differential pressure measurements taken across a static pipe to calculate velocity components normal to the pipe axis. The theory has been developed for circular cross-section pipes in two-dimensional and three-dimensional disturbance fields, and for elliptical cross-section pipes in a two-dimensional disturbance field. This concept gives a rugged and relatively inexpensive measuring system that provides an alternative to LDV, hot-wire systems, or aerodynamic probes for many applications. Wind tunnel experiments are described as an example of application of the concept in a practical experimental situation. The theoretical analysis employed in the concept will require further development to improve the applicability of the concept to the interesting and important case of transonic flow with shock waves.

Acknowledgments

This work was sponsored by the Arnold Engineering Development Center, Air Force Systems Command, United States Air Force under Contract F40600-78-C-0003.

References

[1] Sears, W. R., Vidal, R. J., Erickson, J. C. Jr., and Ritter, A., "Interference-Free Wind-Tunnel Flows by Adaptive-Wall Technology," *Journal of Aircraft*, Vol. 14, Nov. 1977, pp. 1042-1050.

[2] Erickson, J. C. Jr., Wittliff, C. E., and Daughtry, D. C., "Further Investigations of Adaptive Wall Wind Tunnels," Arnold Engineering Development Center Rept. AEDC-TR-80-34, Oct. 1980.

[3] Van Dyke, M. D., *Perturbation Methods in Fluid Mechanics*, Academic Press, New York, 1964.

[4] Churchill, R. V., *Complex Variables and Applications*, 2nd ed., McGraw-Hill, New York, 1960.

[5] Sears, W. R., "Self-Correcting Wind Tunnels," The Sixteenth Lanchester Memorial Lecture, *The Aeronautical Journal*, Vol. 78, Feb./March 1974, pp. 80-89.

[6] Vidal, R. J., Erickson, J. C. Jr., and Catlin, P. A., "Experiments With a Self-Correcting Wind Tunnel," Wind Tunnel Design and Testing Techniques, AGARD-CP 174, Oct. 1975, pp. 11-1 to 11-13.

[7] Vidal, R. J. and Erickson, J. C. Jr., "Research on Adaptive Wall Wind Tunnels," Arnold Engineering Development Center Rept. AEDC-TR-78-36, Nov. 1978.

[8] Murman, E. M., Bailey, F. R., and Johnson, M. L., "TSFOIL—A Computer Code for Two-Dimensional Transonic Calculations, Including Wind-Tunnel Wall Effects and Wave-Drag Evaluation," Paper 26, *Aerodynamic Analyses Requiring Advanced Computers*, NASA-SP-347-Pt. 2, March 1975.